



### 1. Motivation

The scrape-off-layer (SOL) heat-flux width  $\lambda_q$  is a key parameter governing power exhaust in magnetic confinement devices, making its accurate characterization essential for predicting divertor heat loads and optimizing power handling.

While extensive experimental studies in tokamaks have established robust empirical scaling laws yielding  $\lambda_q \propto B_{pol}^{-1.19 \pm 0.08}$  [1], exhibiting only weak dependence on  $P_{SOL}$ ,  $R$  and  $B_{tor}$ ,  $\lambda_q$  scaling in stellarators remains insufficiently characterized.

This reflects the limited availability of dedicated stellarator experimental datasets spanning diverse operational regimes. Predictive power exhaust capability for stellarator reactor design requires multi-machine mapping of  $\lambda_q$  along field lines from the upstream SOL to PFCs, including limiter configurations such as TJ-II or island divertor configurations as in W7-X and LHD.

### 1. Project objectives and methodology

This poster introduces the project framework for studying  $\lambda_q$  and SOL turbulence scaling in stellarators, along with the first experimental activities conducted at the TJ-II stellarator.

The methodology combines dedicated experimental measurements and numerical modelling.

Experimentally, the objective is to investigate the dependence of  $\lambda_q$  and SOL turbulence on magnetic field strength, heating power and plasma density.

The experimental characterization will support the validation of reduced SOL transport modelling, with the ultimate goal of improving predictive capabilities for heat-flux deposition on PFCs.

The experimental programme relies primarily on radial Langmuir probe (LP) measurements to characterize upstream SOL profiles of  $n_e$ ,  $T_e$  and  $\phi$  as well as  $n_e$  and  $\phi$  fluctuations.

Through EMC3-Lite [2] and physics-informed neural networks (PINNs) [3], both constrained by anisotropic heat transport equations.

$\lambda_q$  measurements can be used to infer cross-field transport coefficients within the EMC3-Lite framework, while measured radial temperature profiles provide training and validation data for the PINN model.

Infrared thermography complements these measurements to provide power deposition two-dimensional maps at limiter or divertor targets.

Dedicated Langmuir probe (LP) studies were initiated during the 2026 TJ-II spring campaign, and a preliminary analysis of these measurements is presented in this poster. In parallel, experiments using the Multi-Purpose Manipulator (MPM) have been proposed for upcoming W7-X operational phases (OP2.4 and OP2.5).

### 3. Langmuir probe experimental setup

TJ-II is a resistive heliac stellarator with  $R = 1.5\text{m}$ ,  $a \approx 0.2\text{m}$  and  $B_{00} \approx 1\text{T}$ . It has four-period symmetry, with the vessel divided into eight subsectors per period.

The LP system was installed in the D4 subsector, a region with magnetic flux expansion.

- The probe was operated at fixed insertion depths during each discharge. Multi-pin probe heads enabled the simultaneous radial measurements  $I_{sat}$ ,  $V_f$ , triple-probe (TP), or swept  $I-V$  depending on the pin role.
- Two probe heads were used: a rake probe and a podium probe, both with 3 mm radial pin spacing.

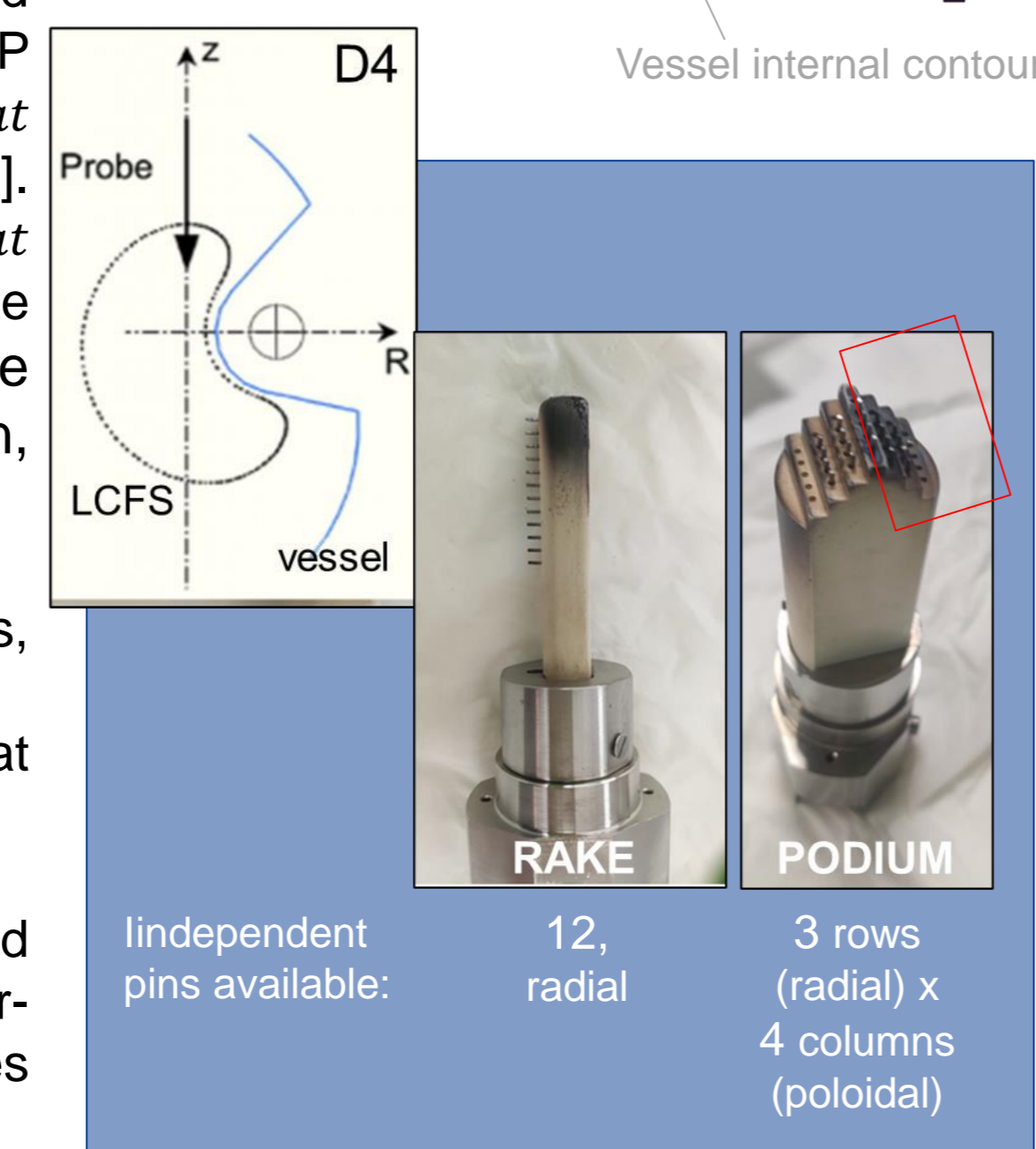
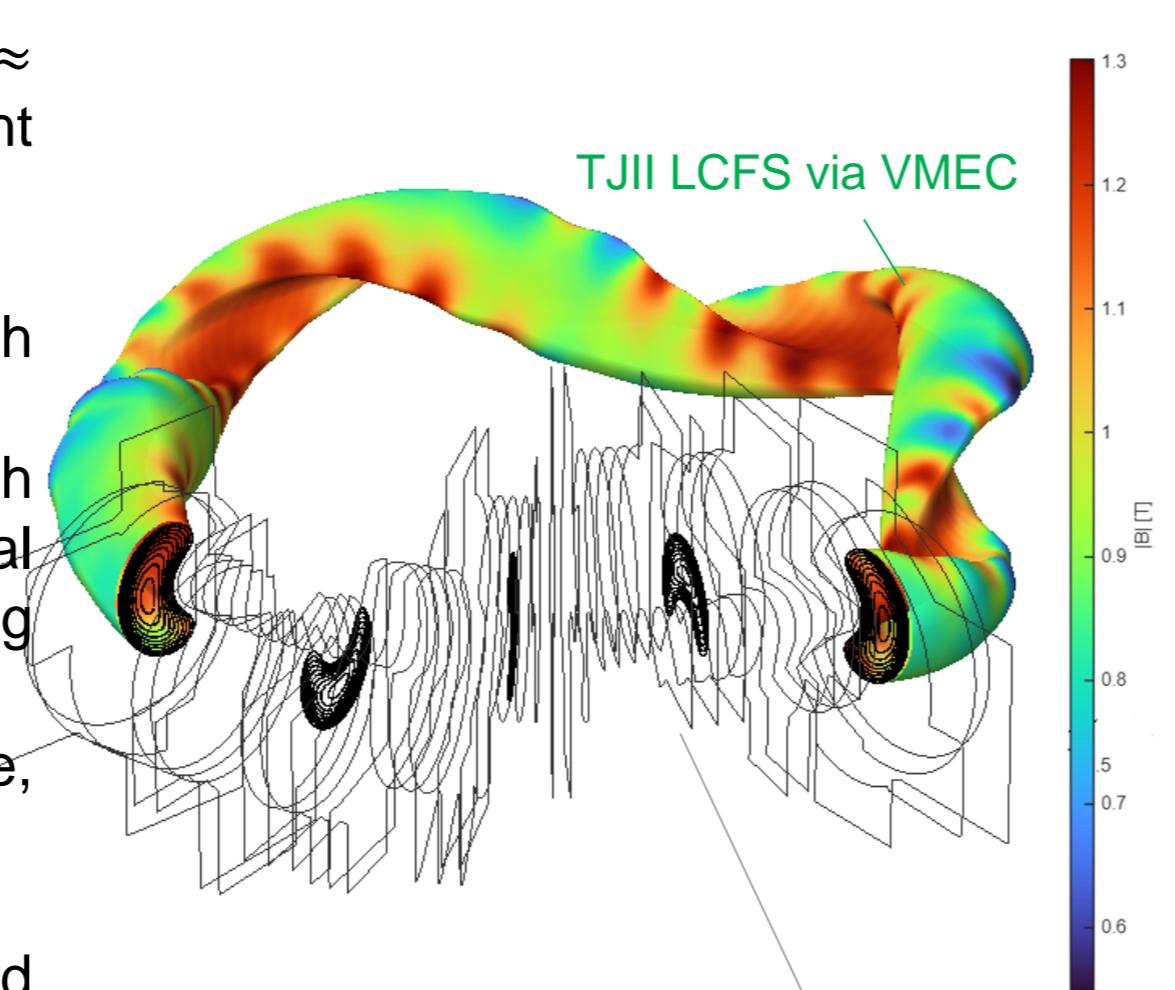
**Analysis methodology:** Plasma properties are derived using standard probe analysis and sheath theory.  $T_e$  is obtained either from TP configurations or swept  $I-V$  characteristics,  $n_e$  is inferred from  $I_{sat}$  using Bohm sheath theory,  $I_{sat} \propto ne\sqrt{T_e}$ , and  $\phi \approx Vf + aTe$  [4]. Turbulence properties are characterized from fluctuations of  $I_{sat}$  current and  $V_f$  signals,  $\tilde{n}_e \approx \tilde{I}_{sat}$  (assuming  $T_e$  fluctuations can be neglected) and  $\tilde{\phi} \approx \tilde{V}_f$ . Characteristic decay lengths are estimated from radial  $T_e$  and  $n_e$  profiles in the SOL region, assuming an exponential fall-off.

**Datasets of interest** belong to three different experiment days, involving:

- ECRH plasmas with power scans between 250–550 kW at nominal magnetic field
- Standard magnetic configuration at nominal field
- Two low-density cases with the lowest  $n_e = 0.5e19\text{ m}^{-3}$  and the highest above the electron-to-ion root transition. A higher-density ECRH+NBI case was also analyzed, reaching densities beyond the ECRH cut-off.

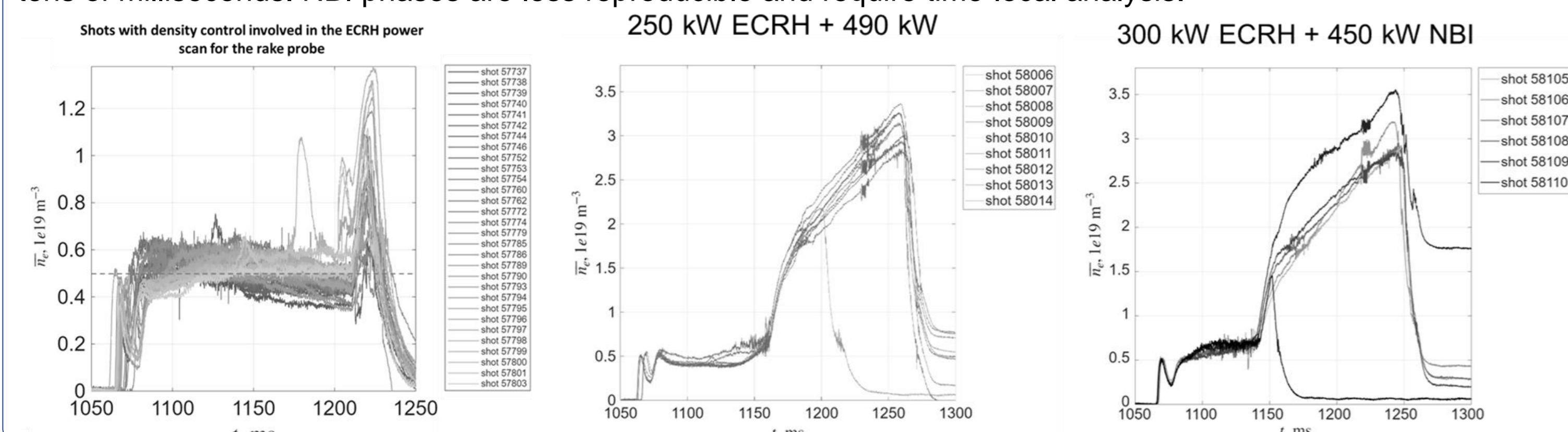
The rake probe was used for ECRH power scans, while the podium probe covered fixed-power ECRH (250, 300 kW) and NBI (450, 490 kW) discharges.

\*) On-axis, X injection and 2nd harmonic; equal power from two 53.2 GHz gyrotrons. \*\*) Only NBI2.



### 4. Discharge characterization

Overall, line-density traces show good density control and reproducible ECRH phases, enabling comparisons over tens of milliseconds. NBI phases are less reproducible and require time-local analysis.



### 5. Preliminary results

Representative measurements of  $I_{sat}$  and  $V_f$  are presented for different density, confinement regime and heating ECRH power conditions. The analysis is based on time-averaged values over the selected time windows. Error bars represent the standard deviation of the signals, and therefore quantify the intrinsic fluctuation level of the measurements around the mean value. No frequency spectral analysis is included at this stage.

An acceptable shot-to-shot reproducibility has been verified for the discharge sets considered in this work. In most cases, the observed differences between nominally identical discharges remain within the fluctuation level of the measurements, allowing the reconstruction of radial profiles from multiple discharges when required. Cases where profiles are assembled from different shots are explicitly indicated.

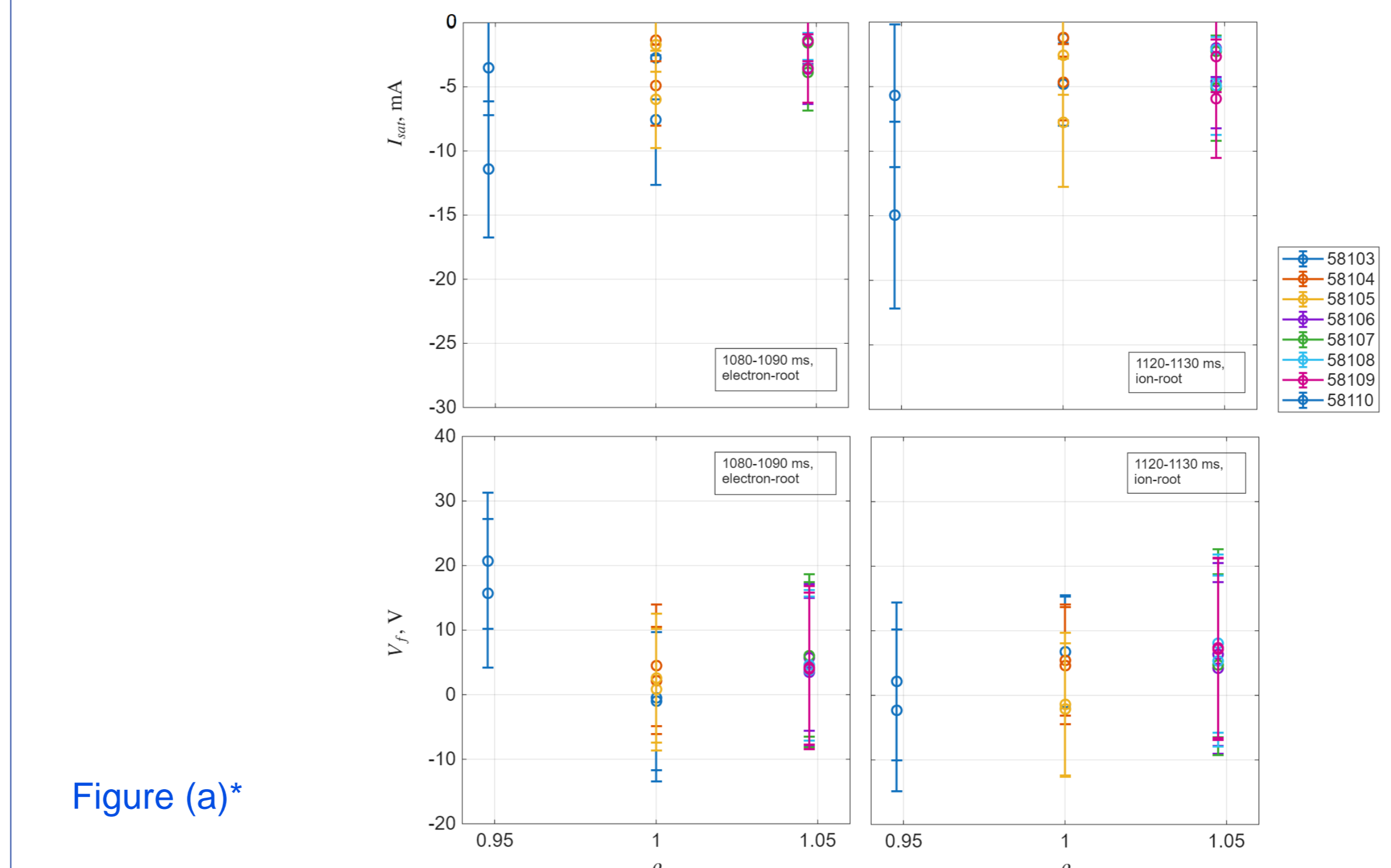


Figure (a)\*

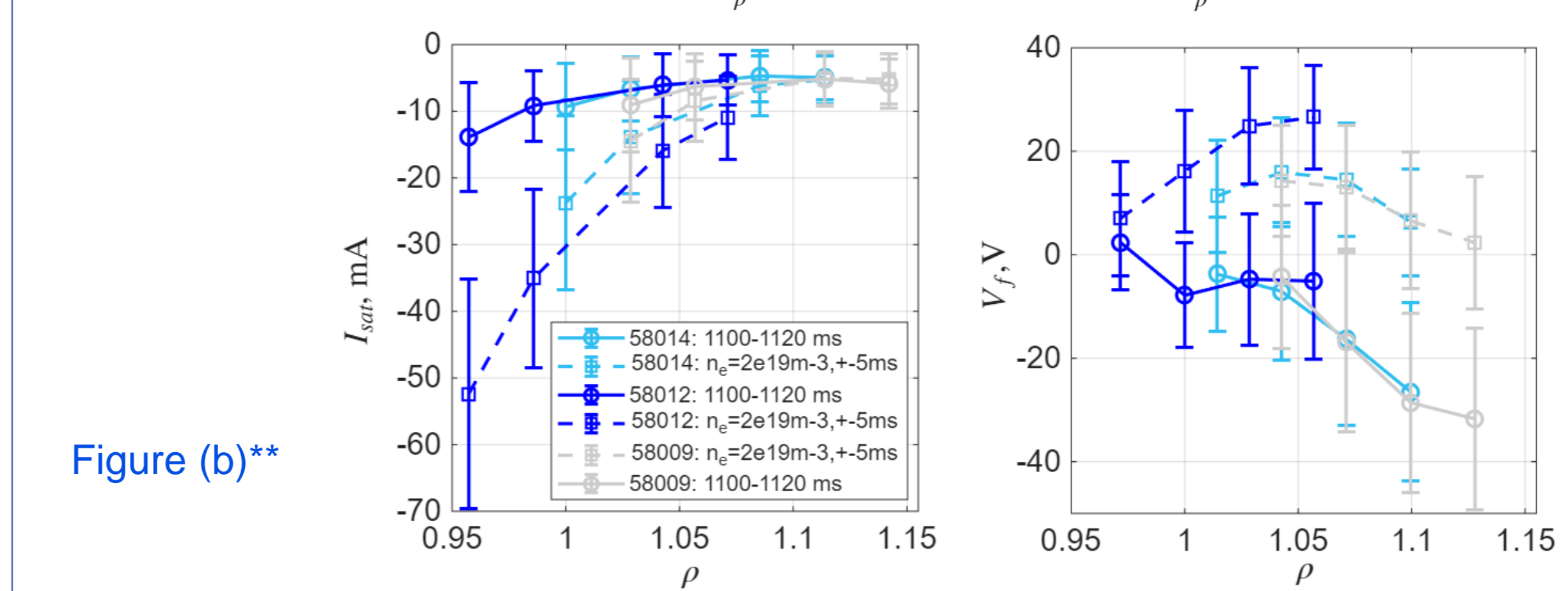


Figure (b)\*\*

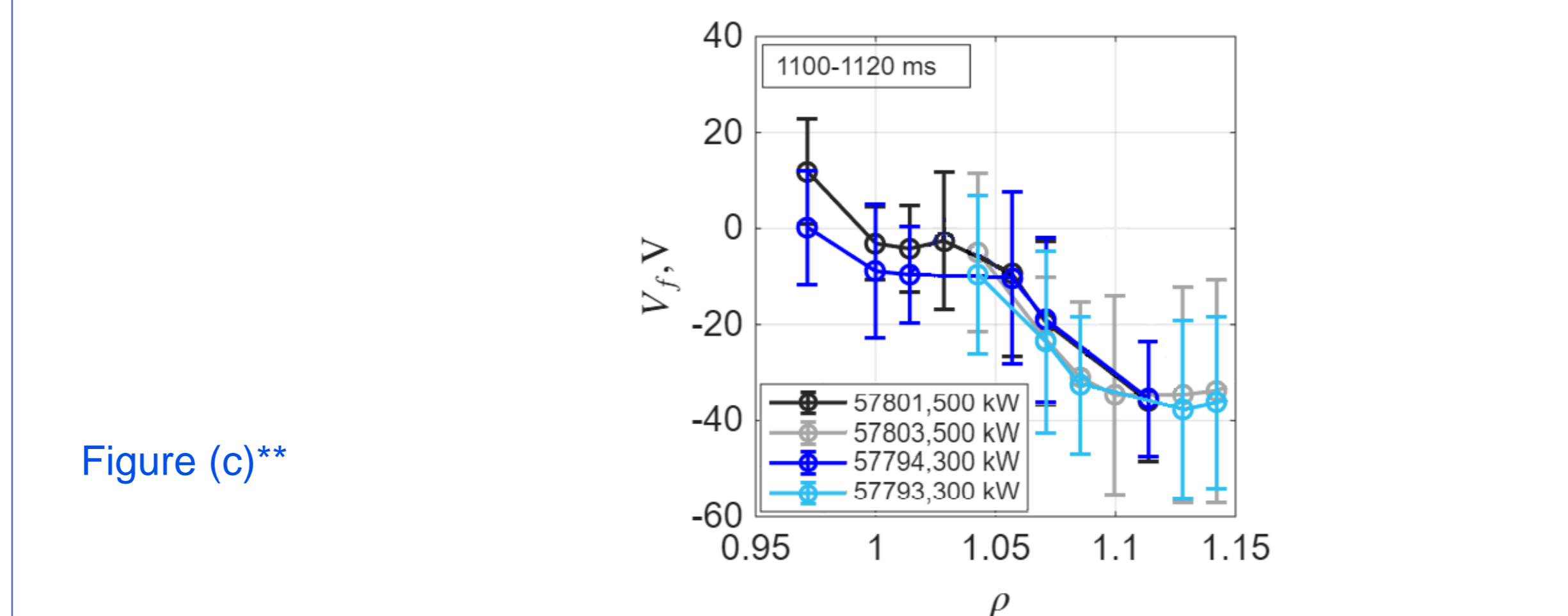


Figure (c)\*\*

A systematic dependence of the Langmuir probe signals on plasma density is observed. The floating potential  $v_f$  (Fig. a, bottom) provides the clearest signature of the electron-to-ion root transition, consistent with the expected reversal of the radial electric field. This effect is most evident inside the estimated LCFS, while its impact in the SOL is more limited.

$I_{sat}$  increases near the LCFS during ECRH operation (Fig. a, top). Similar behaviour is observed during NBI-heated phases (Fig. b, left). In contrast, no significant changes are observed at radial positions approximately 2 cm outside the estimated LCFS.

Previous TJ-II probe studies report lower NBI-driven  $I_{sat}$  in the SOL compared to ECRH plasmas [5]; however, this trend is not observed in the present dataset.

A preliminary power scan is available for  $v_f$ . Fig. c shows representative measurements at two ECRH power levels. Only limited variations of  $v_f$  with heating power are observed, and no clear power scaling can be established at this stage.

\*) For each discharge, only a single pin from the upper row of the planar probe was used in the analysis.  
\*\*) Floating potential raw data close to [50 V] in Fig. (b) and (c) show indications of saturation in the fluctuation amplitude at this voltage due to constraints of the measurement setup.

### 6. Conclusions and future work

In the context of the Langmuir probe diagnostics in TJII:

#### Conclusions

- Preliminary Langmuir probe measurements suggest a dependence of both  $I_{sat}$  and  $V_f$  on plasma density and confinement regime.
- The electron-root to ion-root transition is most clearly reflected in the floating potential profiles, consistent with a modification of the edge radial electric field.
- Only limited power dependence is observed in the present dataset.

#### Next steps

- Characterization of plasma properties, fluctuations, and profile decay lengths.
- Integration of complementary diagnostics for measurement validation.
- Extension of the database to additional operational regimes and parameter ranges.

[1] T. Eich et al 2013 Nucl. Fusion 53 093031  
 [2] Y Feng and W7-X-team 2022 Plasma Phys. Control. Fusion 64 125012  
 [3] J Gallego et al 2026 XL Reunión Biental RSEF. Seville, Spain.  
 [4] Lobbia and Beal 2017 J. Propul. Power 33 566–581  
 [5] G. Grenfell et al 2019 Nucl. Fusion 59 016018

m.scherezade.barquero@ciemat.es